Journal of Alloys and Compounds 705 (2017) 764–768

Contents lists available at ScienceDirect

Journal of Alloys and Compounds

journal homepage: http://www.elsevier.com/locate/jalcom

Evidence of phase transitions in MoO_2 single crystals

L.M.S. Alves [a], F.S. Oliveira [a], B.S. de Lima [a], M.S. da Luz [b, *], A. Rebello [c], S.H. Masunaga [c], J.J. Neumeier [c], C. Giles [d, e], J.B. Leão [f], C.A.M. dos Santos [a]

[a] Universidade de São Paulo, Escola de Engenharia de Lorena, 12602-810, Lorena, Brazil
[b] Universidade Federal do Triângulo Mineiro, Instituto de Ciências Exatas e Tecnológicas, 38064-200, Uberaba, Brazil
[c] Department of Physics, Montana State University, P.O. Box 173840, Bozeman, MT, 59717-3840, USA
[d] Instituto de Física "Gleb Wataghin", UNICAMP, Campinas, SP, C.P. 6165, 13083-970, Brazil
[e] Laboratório Nacional de Luz Síncrotron, CP-6192, 13084-971, Campinas, SP, Brazil
[f] NIST Center for Neutron Research, National Institute of Standards and Technology, Gaithersburg, MD, 20899-8562, USA

ARTICLE INFO

Article history:
Received 12 October 2016
Received in revised form
10 February 2017
Accepted 13 February 2017
Available online 16 February 2017

Keywords:
Phase transition
MoO_2

ABSTRACT

In this work, structural and physical properties are revisited in the MoO_2 compound. MoO_2 single crystals have been prepared by chemical vapor transport technique and characterized by X-ray diffraction, neutron diffraction, high-resolution thermal expansion, electrical resistance measurements, and heat capacity. Electrical resistivity, heat capacity, and thermal expansion measurements show two clear features which are related to phase transitions on the MoO_2 compound. These results suggest that an electronic-type transition occurs near 220 K and a structural transition at ~267 K.

1. Introduction

Molybdenum oxides are well known; nevertheless, they continue to receive extensive attention because of their great stoichiometric and physical properties variety [1–6]. The ideal molybdenum dioxide is monoclinic, weakly paramagnetic, and displays a conventional metallic behavior [7,8]. However, theoretical studies have shown that ultrathin films [9] and bulk with some molybdenum or oxygen vacancies [10] can form magnetic moment with ferromagnetic coupling. The origin of the magnetism observed is still under investigation, but some researchers believe that the reason for that can be related to defects, such as vacancies or interstitial atoms, and low dimensionality effects [10]. Results indicate that small fluctuations of the Mo valences can cause considerable changes in the physical properties of the MoO_x. For instance, it is possible to find compounds with very different physical properties for x between 2 and 3. While MoO_2 has an asymmetric crystalline structure besides Mo-Mo channels along the crystallographic direction a, which results in anisotropic properties [5,11–13], MoO_3 in its more stable phase is orthorhombic and electrically insulating [14–16].

Other binary molybdenum oxides are reported with different chemical contents and oxidation states of Mo, such as Mo_4O_{11}, Mo_8O_{23}, and Mo_9O_{26} [12–17]. All these compounds are very interesting due to their physical properties, showing quasi-low-dimensional transport behavior, transitions related to commensurate and incommensurate states, and formation of CDW instabilities [12,13,18–22]. It was observed in K-doped MoO_2 with critical temperature ranging from 4 to 10 K, depending on the sample composition [23,24]. Furthermore, recently superconductivity was found at 12 K in oxygen-deficient MoO_2 [5].

In this work, electrical resistance, high-resolution X-ray diffractometry, neutron diffraction, high-resolution thermal expansion, and heat capacity are revisited in the MoO_2 compound. These results suggest that an electronic-type transition occurs near 220 K and a structural transition at ~267 K.

2. Experimental procedure

MoO_2 single crystals were grown by chemical vapor transport using $TeCl_4$ as a transporting agent. A quartz tube (length from 150 to 220 mm and inner diameter of 9 mm) containing pure MoO_2 and $TeCl_4$ was sealed under vacuum and introduced into a horizontal resistance furnace provided with three independently controlled heating zones. It was exposed to thermal gradients at temperatures between 650° C and 800° C for 3–7 days.

* Corresponding author.
E-mail address: daluz.mario@icte.uftm.edu.br (M.S. da Luz).

http://dx.doi.org/10.1016/j.jallcom.2017.02.148
0925-8388/

The samples used in this work have typical dimensions of 1.0 mm × 1.5 mm × 0.5 mm with the largest dimension along *a*-axis. Two crystals were polished to obtain rectangular shapes and oriented using back-reflection Laue X-ray diffraction.

Low-resistance gold contacts were deposited on the crystal for measuring the four-probe electrical resistance. Heat capacity measurements were made using a sample platform in which sample was placed in it with "Apiezon N" grease to facilitate thermal contact between the platform and the crystal which weighed 48,35 mg. Both measurements were performed as a function of temperature using a 9 T cryo-free Physical Properties Measurement System (PPMS) from 2 K to 300 K.

Thermal expansion (TE) was measured using a high-resolution capacitive dilatometer cell constructed from fused quartz [25]. TE data were collected in an interval of 0.2 K using a warming rate of 0.20 (1) K/min.

Additionally, high-resolution Synchrotron X-ray powder diffraction was measured using a Shimazu diffractometer (XRD 6000) with 40 kV - 30 mA, Cu Kα radiation, and Ni filter, and at several temperatures in the Brazilian Synchrotron Light Laboratory. Furthermore, neutron powder diffraction data were collected using the BT-1 32 detector neutron powder diffractometer at the NCNR, NBSR. A Cu(311) monochromator with a 90° take-off angle, λ = 1.5403(2) Å, and in-pile collimation of 15 min of arc were used. Data were collected over the range of 3–168° 2θ with a step size of 0.05°. The instrument is described in the NCNR web site [26]. The samples were loaded in vanadium can sample container of 50 mm length and 6.2 mm diameter and sealed under an atmosphere of helium gas. These experiments were performed at room temperature to confirm the monoclinic structure of a high purity commercial MoO_2 (space group $P2_1/c$) sample, and also at several temperatures during warming.

3. Results

Fig. 1 shows the electrical resistivity as a function of temperature measured with applied electrical current along *a*-axis of a MoO_2 single crystal. The resistivity, in the cooling regime, decreases with decreasing temperature as expected for conventional metals and in agreement with previous results [7,8]. In addition, the resistivity values at 0 and 300 K are $2.63.10^{-6}$ Ω cm and $2.5.10^{-4}$ Ω cm which leads to a residual resistivity ratio (RRR) of approximately 95. The hysteresis between cooling and warming resistivity curves near room temperature has been related to a first-order phase transition. Similar hysteresis has been observed in the correlated $K_{0.05}MoO_2$ compound [4].

In the warming regime, two interesting features were observed. There are two changes in the slope, one close to 220 K and another at 267 K, which can be related to two phase transitions. Furthermore, a careful inspection of electrical resistivity under cooling displays a change in the slope near 267 K (shown in Fig. 1 inset). The same behavior has also been observed in three other MoO_2 crystals and, to our best knowledge, these transitions have never been reported.

In order to confirm the occurrence of the two phase transitions, we have also measured high resolution thermal expansion, neutron powder diffractometry, X-ray powder diffraction, and heat capacity as a function of temperature.

Linear thermal expansions (LTE), normalized to the length at 300 K ($\Delta L/L_{300}$) along the crystallographic directions *a*, *b* and *c*, are displayed in Fig. 2(a) (solid symbols). The LTE have the similar general behavior for the three different directions with a small difference in magnitude between them. For all directions, the length of the crystal shrinks with decreasing temperature, as occurs in most of the materials. In the *a* direction, changes in slope close to

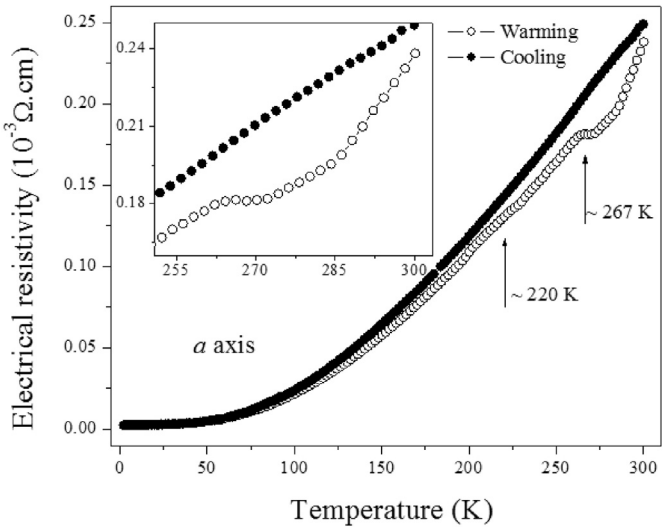

Fig. 1. Electrical resistivity as a function of temperature measured in both warming and cooling regimes along *a*-axis of a MoO_2 single crystal. Arrows indicate the transition temperatures. Inset displays a zooming near the phase transition at ~267 K.

220 K and 267 K have been observed (see Fig. 2(b) and (c), the red lines are guides to the eye). These changes can be better observed using the thermal expansion coefficient, α, calculated from the derivative $1/L_{300}\ d(\Delta L)/dT$ (see Fig. 2(d) and (e)), which show changes in the slope close to 220 K and 267 K. These temperatures can be associated with the occurrence of the second order phase transition observed around 267 K in the electrical resistivity and with its small change at 220 K. Furthermore, similar features can be found in the other two crystallographic directions. In order to check the reproducibility, the high-resolution thermal expansion measurements were repeated along each direction showing similar results (not shown).

Fig. 2 a) also shows the linear thermal expansion calculated from neutron diffraction measurements (open symbols). The agreement between the thermal expansion and neutron diffraction data is good. The difference can be related to the resolution of the techniques. High-resolution thermal expansion can detect 0.1 Å changes in length with a relative resolution of about 10^{-8}, this resolution is at least 4 orders of magnitude higher than what is possible with X-ray or neutron diffraction [25].

The temperature dependence of heat capacity is shown in Fig. 3. Two clear features can be observed in the range 2 K ≤ *T* ≤ 300 K: an increase in C_P close to 220 K (upper panel on the right) and a broad peak, starting at 267 K (lower panel on the right). This seems to agree with the two phase transitions observed in the electrical resistance and thermal expansion measurements shown in previous figures.

At low temperature, a plot of C_P/T versus T^2 allows comparison to the expected behavior $C_P/T = \gamma + \beta T^2$, where γ is the electronic specific heat coefficient and $\beta \propto \theta_D^{-3}$ describes the lattice contribution (see inset in the main panel of Fig. 3). When plotted in this manner, the data exhibit linear behavior in the range $2 < T^2 < 120$ K^2. The fit reveals a value of $\gamma = 1.85\ (3)$ mJ mol^{-1} K^{-2} and $\beta = 0.0315\ (5)$ mJ mol^{-1} K^{-4}, which leads to a Debye temperature of $\Theta_D = 635$ K. For comparison, Debye temperature of 525 K has been reported for MoO_2 polycrystalline samples [4].

Synchrotron X-ray diffraction (XRD) experiments were also performed varying the sample temperature around the phase transition at 267 K upon warming the sample. The results are shown in Fig. 4; the main panel display the results for room temperature (296 K) measurement. All peaks can be indexed as a

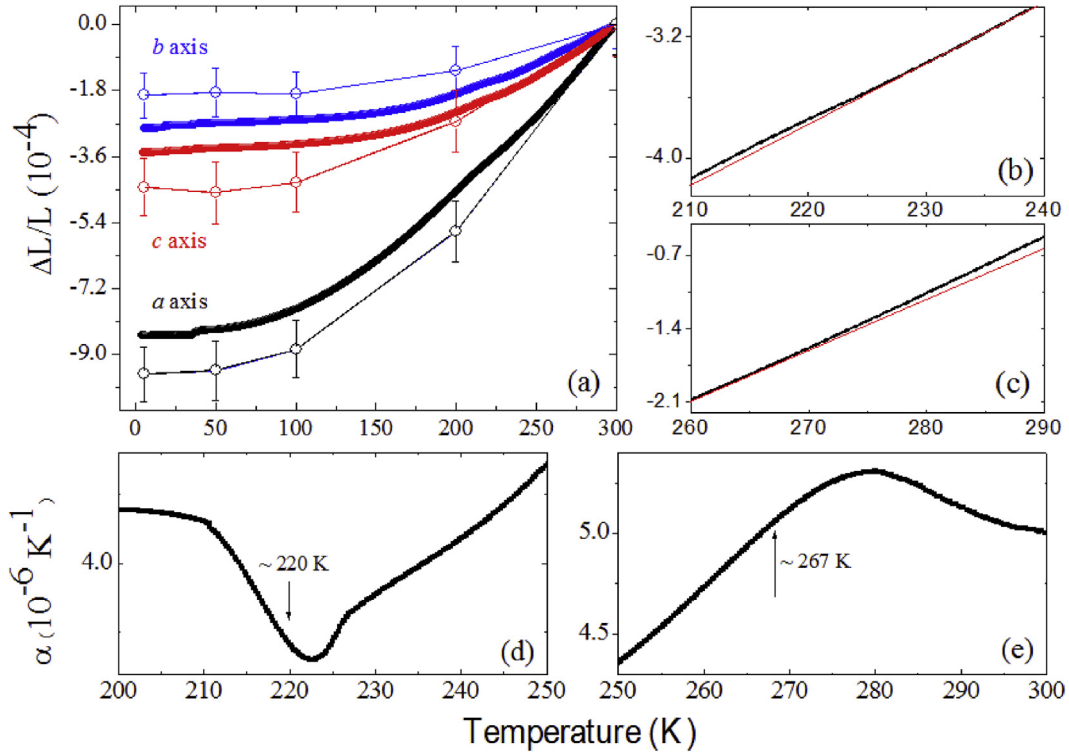

Fig. 2. a) Linear thermal expansion ($\Delta L/L_{300}$) for *a*, *b*, and *c* crystallographic directions. Open symbols show the $\Delta L/L_{300}$ taken from neutron diffraction measurements (b) and (c) show the changes in slope close to 220 K and 267 K for the *a* direction (the red lines are guides to the eye). The thermal expansion coefficient (α), also for the *a* direction is shown in details in (d) and (e) near the phase transition. (For interpretation of the references to colour in this figure legend, the reader is referred to the web version of this article.)

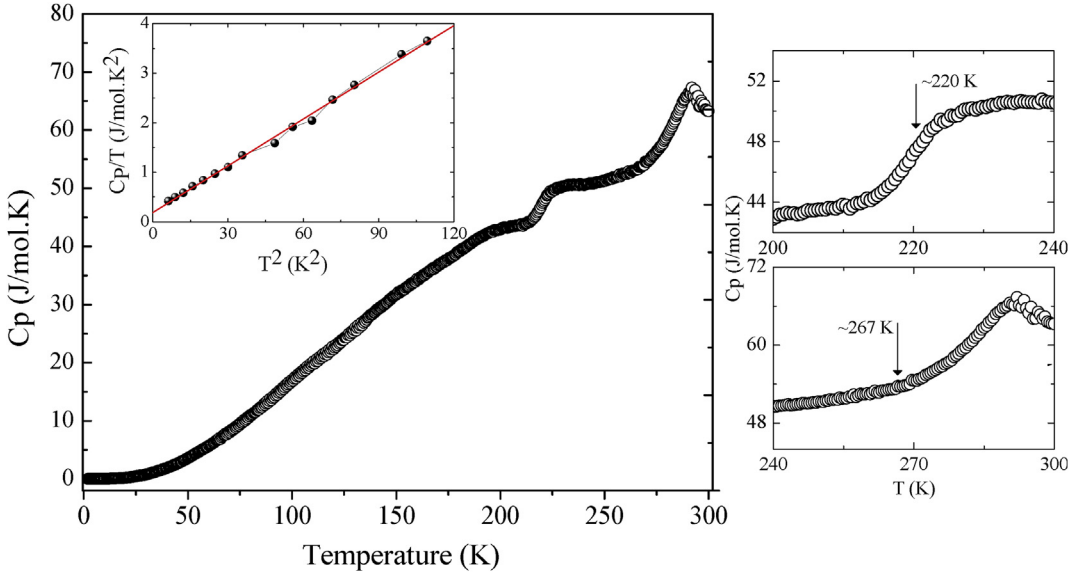

Fig. 3. Specific heat measurement as a function of temperature for a MoO_2 single crystal. The inset shows C_P/T versus T^2 along with the linear fit. The right panels show magnifications near the phase transitions close to 220 K (upper) and 267 K (lower).

monoclinic MoO_2 structure with lattice parameters a = 5,60752(8) Å, b = 4,85779(7) Å, c = 5,62543(8) Å and β = 120,928(1) (χ^2 = 1,810, R_{wp} = 0,0776) belong to space group $P2_1/c$ [12]. The evolution of selected powder X-ray diffraction peaks (indicated by arrows in the main panel) as a function of temperature in the 2θ range from 25.5° to 26.3° (a), from 40.7° to 43.7° (b), and from 48° to 52° (c) are shown in the insets.

One can observe a shift and split into two peaks in the XRD at 240 K and 250 K as shown in the inset 4 a). Furthermore, some peaks at room temperature simply vanish by decreasing the temperature (see insets 4 b) and 4 c)). These features clearly demonstrate that a structural phase transition takes place between room temperature and 250 K in the MoO_2 compound. However, we are not able to determine which crystalline structure is formed at temperatures below ~267 K. The available data do not allow us to define the low temperature phase. Furthermore, the neutron

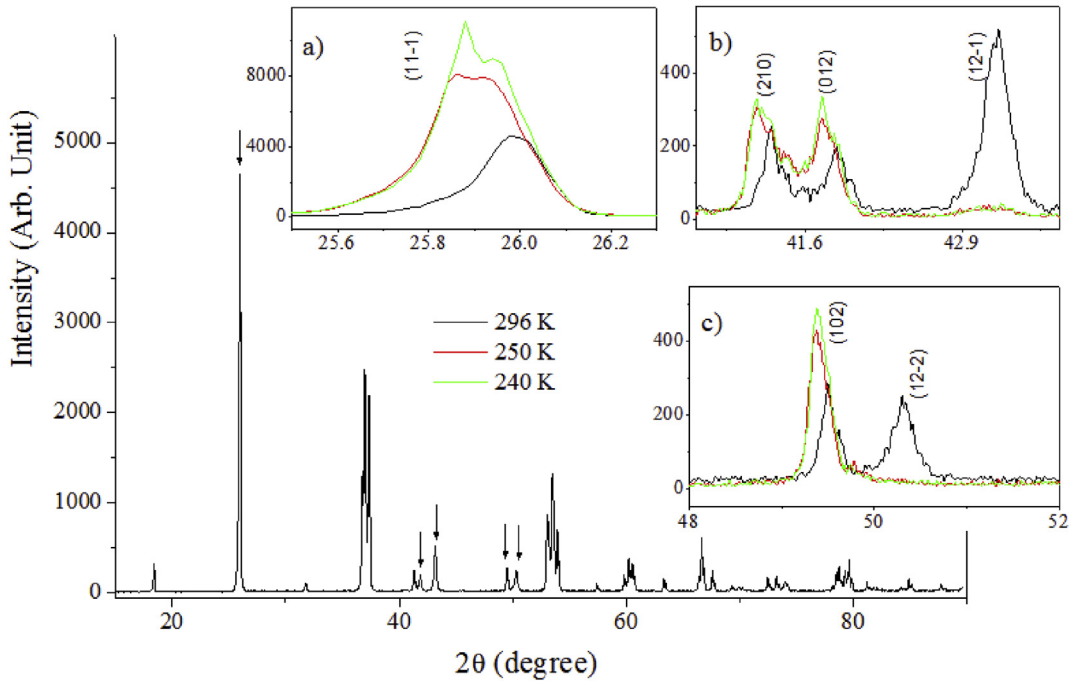

Fig. 4. High-resolution Synchrotron powder diffraction for the MoO_2 at three different temperatures. The inset shows the evolution of selected powder XRD patterns as a function of temperature in the 2θ range from a) 25.5° to 26.3°, from b) 40.7° to 43.7°, and from c) 48° to 52°.

diffraction data refinement suggests that the 220 K phase transition is not structural in nature.

Finally, structural phase transitions (polymorphism) has been reported in other metal-dioxides such as SiO_2, GeO_2, TiO_2, MnO_2, PbO_2 and ReO_2 [7]. The last one below about 300 °C is monoclinic like MoO_2. Cooling about 300 °C this compound changes to an orthorhombic structure characterized by zigzag chains of Re atoms along *c*-axis [7]. Similar structural transition from monoclinic to orthorhombic can be related to the phase transition observed near room temperature in MoO_2. To confirm these assumption further structural experiments need to be done.

4. Conclusion

Electrical resistivity, heat capacity, and thermal expansion measurements show two clear features near 220 K and 267 K suggesting two phase transitions in MoO_2 compound.

The transition at ~267 K has been related to a structural phase transition in the MoO_2 by high resolution synchrotron X-ray diffratometry measurements. Low temperature neutron diffraction measurements suggest that the phase transition is electronic or magnetic in nature. The origin of both transitions is still under investigation.

Acknowledgments

This work is based upon work supported by the FAPESP (2009/54001-2 and 2010/06637-2) and CNPq (448041/2014-6, 300821/2012-3, 303429/2015-1 and 237050/2012-9) M. S. da Luz also thanks to CAPES and FAPEMIG for financial support. Work at Montana State University was supported by the National Science Foundation (USA) under Contract No. DMR0907036.

We acknowledge the support of the National Institute of Standards and Technology, U. S. Department of Commerce, in providing the neutron research facilities used in this work.

The identification of any commercial product or trade name does not imply endorsement or recommendation by the National Institute of Standards and Technology.

References

[1] V. Storbrt, M. Abbate, L.M.S. Alves, C.A.M. dos Santos, R.J.O. Mossanek, X-ray spectroscopy and electronic structure of MoO_2, J. Alloys Compd. 691 (2017) 138–143.
[2] N. Becker, R. Dronskowski, A First-principles study on new high-pressure metastable polymorphs of MoO_2, J. Solid State Chem. 237 (2016) 404–410.
[3] L.M.S. Alves, S.S. Benaion, C.M. Romanelli, C.A.M. dos Santos, M.S. da Luz, B.S. de Lima, F.S. Oliveira, A.J.S. Machado, E.B. Guedes, M. Abbate, R.J.O. Mossanek, Electrical resistivity in non-stoichiometric MoO_2, Braz. J. Phys. 45 (2015) 234–237.
[4] L.M.S. Alves, B.S. de Lima, C.A.M. dos Santos, A. Rebello, S.H. Masunaga, J.J. Neumeier, J. Leão, Phase transitions in K-doped MoO_2, J. Appl. Phys. 115 (2014) 204912.
[5] D. Parker, J.C. Idrobo, C. Cantoni, A.S. Sefat, Evidence for superconductivity at T_c=12 K in oxygen-deficient $MoO_{2-\delta}$ and properties of molybdenum arsenide and oxide binaries, Phys. Rev. B 90 (2014) 054505.
[6] N. Dukstiene, D. Sinkeviciute, Photoelectrochemical properties of MoO_2 thin films, J. Solid State Electrochem. 17 (2013) 1175–1184.
[7] L. Ben-Dor, Y. Shimony, Crystal-structure, magnetic-susceptibility and electrical-conductivity of pure and NiO-doped MoO_2 and WO_2, Mat. Res. Bull. 9 (1974) 837–844.
[8] D.B. Rogers, R.D. Shannon, A.W. Sleight, J.L. Gillson, Crystal chemistry of metal dioxides with rutile-related structures, Inorg. Chem. 8 (1969) 841.
[9] J. Nisar, X.Y. Peng, R. Ahuja, Origin of ferromagnetism in molybdenum dioxide from ab initio calculations, Phys. Rev. B 81 (2010) 012402.
[10] F.G. Wang, Z.Y. Pang, L. Lin, S.J. Fang, Y. Dai, S.H. Han, Origin of magnetism in undoped MoO_2 studied by first-principles calculations, Phys. Rev. B 81 (2010) 134407.
[11] L. Kihlborg, Studies on molybdenum oxides, Acta Chem. Scand. 13 (1959) 954–962.
[12] B.G. Brandt, A.C. Skapski, A refinement of crystal structure of molybdenum dioxide, Acta Chem. Scand. 21 (1967) 661.
[13] V. Eyert, R. Horny, K.-H. Höock, S. Horn, Embedded Peierls instability and the electronic structure of MoO_2, J. Phys. Condens. Matter 12 (2000) 4923–4946.
[14] S.O. Akande, A. Chroneos, M. Vasilopoulou, S. Kennou, U. Schwingenschlögl, Vacancy formation in MoO3: hybrid density functional theory and photo-emission experiments, J. Mater. Chem. C 4 (2016) 9526–9531 (and references there in).
[15] D.O. Scanlon, G.W. Watson, D.J. Payne, G.R. Atkinson, R.G. Egdell, D.S.L. Law, Theoretical and experimental study of the electronic structures of MoO_3 and MoO_2, J. Phys. Chem. C 114 (2010) 4636–4645.
[16] G. Andersson, A. Magneli, On the crystal structure of molybdenum trioxide,

Acta Chem. Scand. 4 (1950) 793–797.
[17] M. Greenblatt, Molybdenum Oxide bronzes with quasi-low-dimensional properties, Chem. Rev. 88 (1988) 31–53.
[18] L. Kihlborg, Crystal structure studies on monoclinic and orthorhombic Mo_4O_{11}, Ark. Kemi 21 (1963) 365.
[19] M. Ghedira, H. Vincent, M. Marezio, J. Marcus, G. Furcaudot, Crystalline-structure of the bidimensional metallic conductor Mo_4O_{11}-gamma, J. Sol. State Chem. 56 (1985) 66–73.
[20] M. Sato, H. Fujishita, S. Sato, S. Hoshino, Structural transition in Mo_8O_{23}, J. Phys. C. Solid State Phys. 19 (1986) 3059–3067.
[21] M. Sato, M. Onoda, Y. Matsuda, Structural transition in Mo_NO_{3-N} (N= 9 and 10), J. Phys. C. Solid State Phys. 20 (1987) 4763–4771.
[22] H. Guyot, C. Escribe-Filippini, G. Fourcaudot, K. Konate, C. Schlenker, Charge-density wave instabilities in the quasi-2-dimentional metal eta-Mo_4O_{11}, J. Phys. C. Solid State Phys. 16 (1983) 1227–1232.
[23] L.M.S. Alves, V.I. Damasceno, C.A.M. dos Santos, A.D. Bortolozo, P.A. Suzuki, H.J. Izario Filho, A.J.S. Machado, Z. Fisk, Unconventional metallic behavior and superconductivity in the K-Mo-O system, Phys. Rev. B 81 (2010) 174532.
[24] L.M.S. Alves, C.A.M. dos Santos, S.S. Benaion, A.J.S. Machado, B.S. de Lima, J.J. Neumeier, M.D.R. Marques, J. Albino Aguiar, R.J.O. Mossanek, M. Abbate, Superconductivity and magnetism in the $K_xMoO_{2-delta}$, J. Appl. Phys. 112 (2012) 073923.
[25] J.J. Neumeier, R.K. Bollinger, G.E. Timmins, C.R. Lane, R.D. Krogstad, J. Macaluso, Capacitive-based dilatometer cell constructed of fused quartz for measuring the thermal expansion of solids, Rev. Sci. Instrum. 79 (2008) 033903.
[26] https://www.ncnr.nist.gov/instruments/bt1/.